22. M. Hanfland, K. Syassen, S. Fahy, S. G. Louie, M. L. Cohen, *Phys. Rev. B* **31**, 6896 (1985).
23. I. V. Aleksandrov, A. F. Goncharov, A. N. Zisman, S. M. Stishov, *Sov. Phys. J. Exp. Theor. Phys. Lett.* **66**, 384 (1987).
24. D. Schiferl *et al.*, *J. Appl. Phys.* **82**, 3256 (1997).
25. T. S. Duffy, W. L. Vos, C.-S. Zha, R. J. Hemley, H. K. Mao, *Science* **263**, 1590 (1994).
26. H. K. Mao, P. M. Bell, *Science* **203**, 1004 (1979).
27. S. Merkel, R. J. Hemley, H. K. Mao, *Appl. Phys. Lett.* **74**, 656 (1999).
28. R. J. Nelmes *et al.*, *Phys. Rev. Lett.* **81**, 2719 (1998).
29. P. Link, I. N. Goncharenko, J. M. Mignot, T. Matsumura, T. Suzuki, *Phys. Rev. Lett.* **80**, 173 (1998).
30. S. H. Lee, M. S. Conradi, R. E. Norberg, *Rev. Sci. Instrum.* **63**, 3674 (1992).
31. W. A. Bassett *et al.*, in *Proceedings of International Conference AIRAPT-16 and HPCJ-38 on High Pressure Science and Technology*, vol. 7 of *The Review of High Pressure Science and Technology* (Japan Society of High Pressure Science and Technology, Kyoto, 1998), pp. 142–144.
32. B. Li, R. C. Liebermann, D. J. Weidner, *Science* **281**, 675 (1998).
33. Supported by the Center for High Pressure Research grant of NSF.

26 July 2000; accepted 19 September 2000

Förster Energy Transfer in an Optical Microcavity

Piers Andrew* and William L. Barnes

By studying the transfer of excitation energy between dye molecules confined within an optical microcavity, we demonstrate experimentally that Förster energy transfer is influenced by the local photonic mode density. Locating donor and acceptor molecules at well-defined positions allows the transfer rate to be determined as a function of both mutual separation and cavity length. The results show that the Förster transfer rate depends linearly on the donor emission rate and hence photonic mode density, providing the potential to control energy transfer by modification of the optical environment.

Processes involving the interaction between light and matter are fundamental to much of science. An important example is the transfer of excitation energy from an excited donor molecule to an acceptor molecule through the resonant dipole-dipole interaction (RDDI). In addition to its key role in photosynthesis (*1*, *2*), this process is of increasing importance as a means of improving the functionality and efficiency of light-emitting diodes and lasers based on organic materials (*3*, *4*). Control of the spontaneous emission of light is accomplished by the use of structures in which the photonic mode density (PMD) is altered, thus manipulating the optical modes into which emission may take place (*5*, *6*). A wealth of research based on this concept is found within the areas of cavity quantum electrodynamics (*7*) and photonic band gap materials (*8*), and it would be of great interest if one could similarly enhance energy transfer. Here, we demonstrate that such enhancement is possible for the Förster transfer process by studying the transfer of excitation energy between molecules confined within an optical microcavity.

The physical nature of the excitation energy transfer mechanism depends on the donor-acceptor separation, d. When the donor and acceptor are far apart ($d > \lambda/10$), transfer is radiative, coupling being mediated by a real photon. In contrast, when donor and acceptor are close, transfer is nonradiative, being mediated by a virtual photon, a process known as Förster transfer (*9*). Both processes involve interactions between the dipole moments of the donor and acceptor molecules (*10*); the radiative process proceeds through the dipole far field, whereas nonradiative transfer occurs through the evanescent near-field components.

Various theoretical investigations have examined how the RDDI is modified by confined geometries such as microcavities (*11*–*13*) and periodic structures (*14*, *15*). They predict that the PMD affects the RDDI, the strength of the effect dependent on the donor-acceptor separation. Recent experiments on microcavities containing donors and acceptors in well-defined and widely separated positions ($\sim\lambda/4$) have demonstrated control over the radiative transfer process (*16*). To investigate the nonradiative Förster process requires a much reduced separation between donor and acceptor molecules. Hopmeier *et al.* (*17*) studied transfer between donors and acceptors randomly distributed throughout a cavity, observing increased acceptor emission when the transfer energy was resonant with a cavity mode. However, because Förster transfer depends strongly on the donor-acceptor separation, they were unable to draw any conclusions about the influence of the cavity on the nonradiative transfer process. The absence of appropriate experimental information leaves open the question of whether Förster transfer can be controlled by the local optical environment.

To explore this question, we measured energy transfer between monomolecular layers of donor and acceptor molecules separated by known distances contained within a series of microcavity structures. Locating donors and acceptors at fixed positions within the microcavity structure ensured that the molecules experienced the same PMD. We show that transfer is by the Förster process and that the transfer rate depends on the PMD, demonstrating that modification of the local optical environment can be used to control the Förster transfer process.

The length scale associated with the Förster process is called the critical distance and corresponds to the donor-acceptor separation for which the transfer rate equals the sum of all other donor decay rates, of order 5 nm. Because of this small characteristic distance, we need molecular resolution in the position of the donor and acceptor molecules, which we achieved using the Langmuir-Blodgett technique. This monomolecular deposition technique allows fabrication of microcavities in which cavity length, donor-acceptor separation, and position within the cavity can be specified with molecular precision. To clarify the effect of PMD on Förster transfer, we used a donor with monochromatic emission, ensuring a single transfer wavelength. This was achieved by the use of a Eu^{3+} complex [*N*-hexadecyl pyridinium tetrakis (1,3-diphenyl-1,3-propandionato) europium (III)] as the donor molecule because the electric dipole transition at 614 nm has a width of only ~5 nm and the long lifetime (~1 ms) allows accurate dynamic measurements of the transfer process. The acceptor, 1,1′-dioctadecyl-3,3,3′,3′-tetramethylindodicarbocyanine, has a high absorption coefficient at the donor emission wavelength, allowing very efficient transfer to take place. The relevant absorption and emission spectra are given in Fig. 1. The combination of high absorption and excellent spectral overlap results in an extremely large critical transfer distance (~14 nm), ensuring that we can measure the distance dependence of the transfer with sufficient spatial resolution by intercalation of monomolecular spacer layers (thickness = 2.6 nm) between donor and acceptor layers.

The energy transfer system that we used consisted of donor and acceptor monolayers separated by zero, two, four, six, and eight layers, respectively, of a transparent material, 22-tricosenoic acid. The strong distance dependence of the Förster process means that transfer from the donor occurs predominantly to the nearest acceptor. To ensure that the donor–nearest acceptor separation coincided with the donor-acceptor layer separation, we had to use highly condensed acceptor monolayers (area per molecule ~1 nm^2). In this way, we could vary the separation between donors and acceptors from 0 to 25 nm in a carefully controlled manner. A consequence of the highly condensed acceptor layer is that the acceptor emission is strongly self quenched and we were

Thin Film Photonics Group, School of Physics, University of Exeter, Exeter, EX4 4QL, UK.

*To whom correspondence should be addressed. E-mail: pandrew@exeter.ac.uk

unable to obtain time-resolved measurements of acceptor emission.

To provide a wide range of PMDs, we examined this energy transfer system located centrally within three types of microcavity structure. Initially, a weak-cavity control sample was fabricated, comprising the energy transfer system bounded by extra 22-tricosenoic acid layers forming a dielectric slab 130 nm thick (Fig. 2A). Half-cavity structures were formed by depositing the same system on top of a 25-nm-thick silver mirror thermally evaporated onto a silica slide (Fig. 2B). A number of half-cavity structures, of cavity lengths l = 100 to 200 nm, were made by varying the number of 22-tricosenoic acid layers bounding the energy transfer system. After acquiring time-resolved data, full microcavities were fashioned by the evaporation of a second, 20-nm-thick silver mirror on top of the half-cavity samples (Fig. 2C). The cavity lengths were chosen to sweep the resonance wavelength of the full microcavity through the energy transfer wavelength, thus maximizing the range of PMDs available with this structure. Confirmation that these different structures exhibit a wide range of PMDs is provided by the donor-only decay transients (Fig. 2D), acquisition of which is described below. These data show that the spontaneous emission lifetime of the donor changes by a factor of ~2.5 across the range of microcavities used, indicating a commensurate change in the PMD (*18*). The mirror thicknesses used provide good confinement for the waveguide modes, while being thin enough to allow emission to be observed and the cavity modal dispersion to be determined by transmission measurements (*19*).

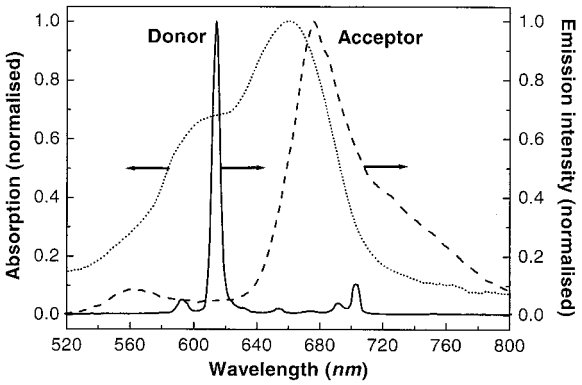

Fig. 1. Spectroscopic data for the donor and acceptor materials. The solid line is the donor emission spectrum; the dotted and dashed lines are the acceptor absorption spectrum and emission spectrum, respectively. These normalized spectra were measured for samples comprising a monolayer of the relevant dye positioned centrally within a dielectric slab ~130 nm thick on a silica slide. Emission spectra were measured after excitation at 337 nm.

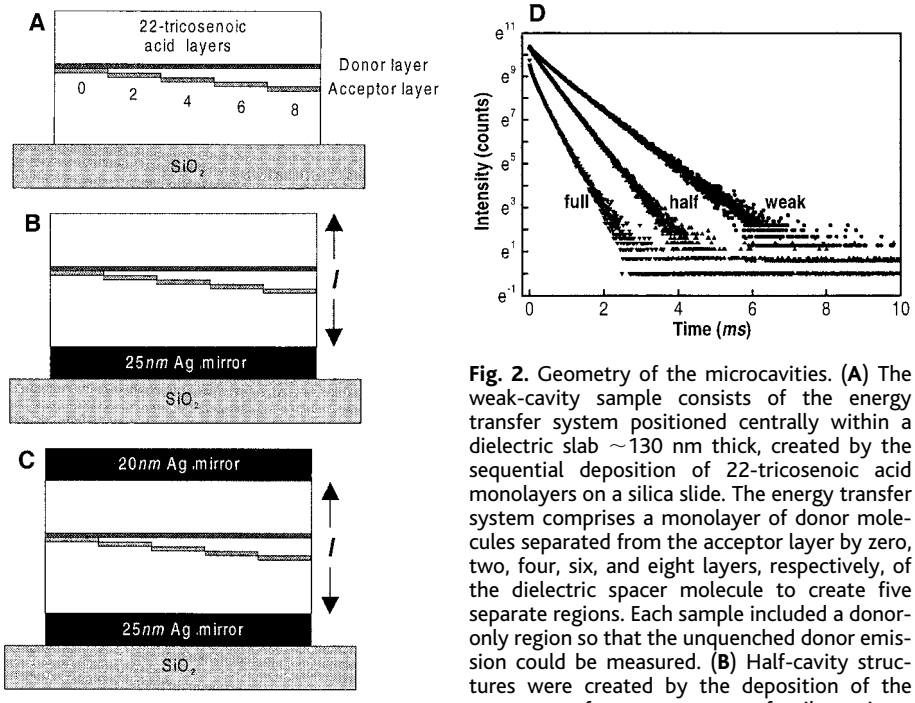

Fig. 2. Geometry of the microcavities. (**A**) The weak-cavity sample consists of the energy transfer system positioned centrally within a dielectric slab ~130 nm thick, created by the sequential deposition of 22-tricosenoic acid monolayers on a silica slide. The energy transfer system comprises a monolayer of donor molecules separated from the acceptor layer by zero, two, four, six, and eight layers, respectively, of the dielectric spacer molecule to create five separate regions. Each sample included a donor-only region so that the unquenched donor emission could be measured. (**B**) Half-cavity structures were created by the deposition of the energy transfer system on top of a silver mirror. Various cavity lengths were constructed by the deposition of extra 22-tricosenoic acid layers. (**C**) Evaporation of a second silver mirror on the top of the half-cavity sample forms the full-cavity sample. (**D**) The temporal decay of the unquenched donor emission at 614 nm for different microcavity samples, illustrating the range of PMDs probed. From left to right, the data correspond to full, half, and weak cavities, each of cavity length ~130 nm. The fitted average lifetimes are τ = 0.26, 0.40, and 0.65 ms.

Our experiment consisted of quantifying the quenching of the donor emission by the acceptor as a function of their separation. We achieved this by measuring the dependence of the donor emission lifetime on the separation distance. A photon-counting technique was used to measure the donor lifetime; donors were excited with a N_2 laser (337 nm, 5-ns pulses), and their emission at 614 nm was spectrally isolated and detected with a cooled photomultiplier tube. The plurality of acceptor molecules in the vicinity of each donor resulted in nonexponential temporal decay traces. Fitting to a multiexponential functional form with a nonlinear least squares fitting routine allowed the average lifetime to be calculated from a weighted average of the lifetime components. The donor emission decay curves shown in Fig. 3A illustrate the increase in donor quenching as the donor-acceptor separation is reduced. The cavity is identical for each of these measurements, save for variation in the acceptor position, ensuring that the donor quenching is only due to a change in the degree of transfer to the acceptor. Furthermore, the PMD is constant (to <5%) for all donor-acceptor separations studied, as confirmed by numerical modeling.

Förster transfer theory predicts the quenching to have an inverse fourth power dependence on layer separation; this was confirmed for a similar transfer geometry by Kuhn *et al.* (*20*). Our samples also exhibited this behavior (Fig. 3B) and from these quenching data, we determined the critical distance, d_0, by fitting the appropriate functional form to our data, Eq. 1.

$$\tau_{DA} = \frac{\tau_D}{1 + (d_0/d)^4} \quad (1)$$

Here, τ_{DA} is the lifetime of the donor distant d from the acceptor, τ_D is the donor lifetime in the absence of the acceptor, and d_0 is the critical distance. The agreement between our data and the fit obtained from Eq. 1 demonstrates that the donor quenching observed was due to the Förster process.

To establish the dependence of Förster transfer on PMD, we then determined the critical distance in a similar way for all 12 confining structures studied. The critical distance so obtained is plotted in Fig. 4A as a function of the donor emission rate, Γ_D (= $1/\tau_D$). The use of the donor emission rate as abscissa has two important advantages. First, the donor emission rate is a direct measure of PMD (*18*), and, second, it allows us to compare the results from all cavities on the same axes. To within experimental error, the critical distance is independent of the donor emission rate, with an average value of 14.1 ± 0.6 nm. As the critical distance is the donor-acceptor separation for which the

transfer rate is equal to the sum of all other donor decay rates, our observation of a fixed value for the critical distance implies that the transfer rate must vary linearly with the donor emission rate.

Further insight can be gained by reanalyzing our data to explicitly examine the effect of the cavity on the energy transfer rate Γ_{ET}, obtained from the rate equation for the system derived from Eq. 1:

$$\Gamma_{ET} = \Gamma_{DA} - \Gamma_D = \Gamma_D(d_0/d)^4 \qquad (2)$$

Γ_{DA} is the donor emission rate, d is distance from the acceptor, and Γ_D is the donor emission rate in the absence of the acceptor. Figure 4B shows Γ_{ET} as a function of Γ_D for data corresponding to donor-acceptor separations of four, six, and eight layers from all microcavities. We did not include data for zero- and two-layer separations because the high degree of donor quenching resulted in too low a signal level. A family of lines results, each line corresponding to a fixed donor-acceptor separation. This linear dependence of the transfer rate on the donor emission rate is direct evidence that Förster transfer does depend on the PMD within the cavity. Using Eq. 2, we can extract the critical distance from the gradients of the lines shown in Fig. 4B. For donor-acceptor separations of four, six, and eight monolayers, we find the critical distance to be 13.7 ± 0.4, 13.5 ± 0.4, and 10.0 ± 1.7 nm, respectively, and they are generally in good agreement with the critical distances independently obtained from the quenching curves (Fig. 4A). The comparison for the eight-monolayer separation is not quite as good, however. For such large separations, the transfer probability is small compared with that of direct emission, making the extraction of transfer parameters less reliable.

It is instructive to compare the critical distance measured for transfer within our cavities with the value found with an independent spectroscopic technique. The critical distance in unrestricted planar geometries is given by Kuhn *et al.* (*20*):

$$d_0 = \frac{\alpha\lambda_d}{n}\left(q\int_0^\infty \frac{f_d(\lambda)\varepsilon(\lambda)}{\lambda^4}d\lambda\right)^{\frac{1}{4}} \qquad (3)$$

Here, α is an orientational factor accounting for the distribution of the donor and acceptor dipole moments within the layers, λ_D is the donor emission wavelength, n is the refractive index of the medium, and q is the donor quantum efficiency. The integral represents the spectral overlap of the donor emission spectrum $f_d(\lambda)$ and the acceptor absorption spectrum $\varepsilon(\lambda)$; $f_d(\lambda)$ is normalized such that the integrated intensity is equal to one on the wavelength scale. Using the appropriate values for our system (*21*), we obtain d_0 = 13.9 ± 0.5 nm, in excellent agreement with the experimentally measured values reported above and further confirmation that transfer is due to the Förster process.

We found that the rate of Förster energy transfer between dye molecules contained within microcavities is directly dependent on the cavity PMD. This follows from our demonstration of both the independence of the critical transfer distance and the associated linear dependence of the energy transfer rate on the donor emission rate Γ_D. The link between the transfer rate Γ_{ET} and the cavity PMD at the transfer energy, $\rho(\omega)$, can thus be directly obtained from Fermi's Golden rule as $\Gamma_{ET} \propto \Gamma_D = (\pi/2\hbar^2)|M_{ij}|^2\,\rho(\omega)$ ($|M_{ij}|$ is the matrix element for the donor transition) (*18*). We interpret our results as follows. Placing the donor in a microcavity alters the effective donor oscillator strength, $|M_{ij}|^2\rho(\omega)$. As the Förster transfer process depends directly on the donor oscillator strength (*9*), the microcavity changes the transfer rate between donors and acceptors confined within it. Alternatively, one could say that the donor is dressed by the microcavity.

It is important to identify the different roles that resonant electromagnetic modes play in radiative and nonradiative transfer processes. In a donor-only system, resonant modes provide a strong decay channel and so increase the donor

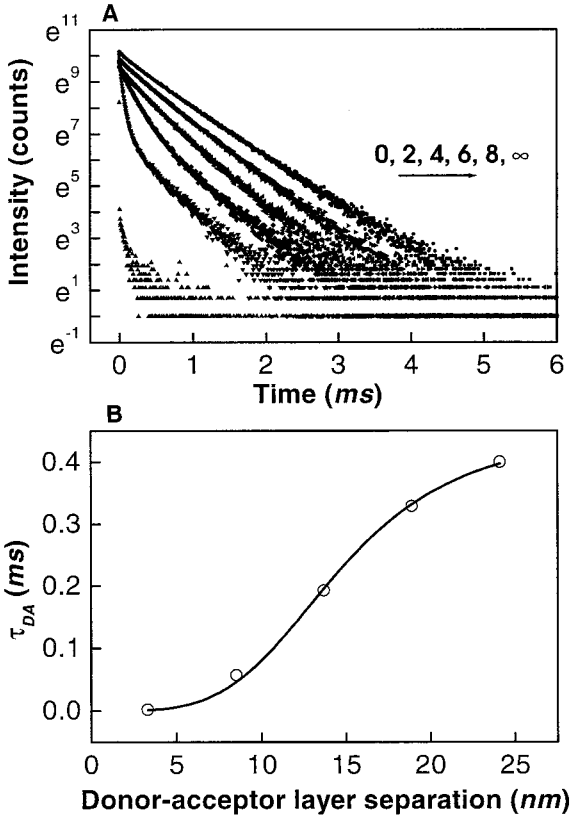

Fig. 3. Quenching of the donor emission by the acceptor layer as a function of the donor-acceptor separation measured for one of the half-cavity samples (cavity length = 200 nm). (**A**) Temporal decay of the donor emission at 614 nm for the various donor-acceptor separations, measured after excitation at 337 nm. The traces correspond to, from left to right, donor-acceptor layer separations of zero, two, four, six, and eight 22-tricosenoic acid spacer layers, respectively. The right-hand trace is for donor decay in the absence of an acceptor layer. In each case, the emission measured is purely due to the donor because acceptor emission is minimal at 614 nm and has a much shorter lifetime (~ns) and can thus discounted. (**B**) Donor lifetime in the presence of an acceptor layer, τ_{DA}, as a function of donor-acceptor layer separation. The lifetimes are obtained from the data in (A) and are represented by the open circles, and the solid line is obtained by fitting Eq. 1 to the data. For this sample, we find d_0 = 14.7 ± 0.3 nm and τ_D = 0.45 ± 0.01 ms. The intensity of the donor emission was also quenched with a $1/d^4$ dependence on the donor-acceptor separation.

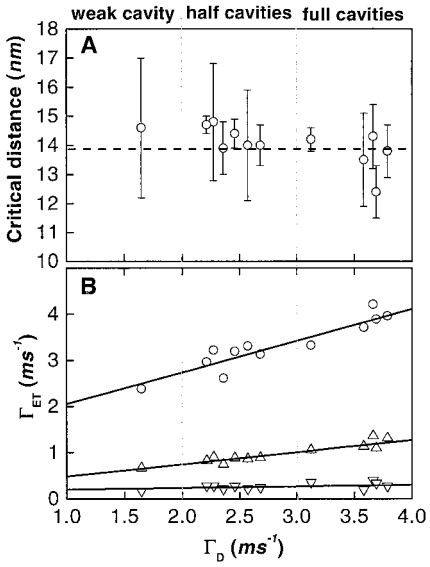

Fig. 4. Dependence of Förster transfer on the donor emission rate. (**A**) Critical distances were determined for the various microcavity structures, and hence donor emission rate, from quenching curves similar to that of Fig. 3B. The open circles with error bars are the experimental data; the dashed line is the value of critical distance predicted for our energy transfer system with Eq. 3. (**B**) Dependence of the Förster energy transfer rate, Γ_{ET}, on the donor emission rate in the absence of acceptors, Γ_D, for all microcavities studied. Data are shown for three donor-acceptor separations, four layers (O), six layers (Δ), and eight layers (∇), together with linear fits for each set of data. The vertical lines divide the data into the three cavity types studied. The data show that the Förster transfer rate depends linearly on the donor emission rate for all donor-acceptor separations.

decay rate, thus effectively increasing the donor oscillator strength. In the nonradiative Förster process, the transfer rate is dependent on this oscillator strength and so is similarly enhanced by the PMD, as shown here. The situation is different for radiative transfer. Because the evanescent donor dipole near-field components are negligible for separations appropriate to radiative transfer, the mode acts directly as a mediator, being the only way of transporting energy from donor to acceptor. This process does not alter the donor decay rate because donor and acceptor are decoupled by the mediating photon. This situation was studied by Folan *et al.* (*22*), who investigated transfer between donors and acceptors positioned on the surface of a microdroplet. Enhanced acceptor emission was observed because of a two-stage process; the donor excited a Mie resonance of the droplet, which was in turn damped by excitation of the acceptor. The high field strength associated with the Mie resonance allowed efficient transfer over large donor-acceptor separations (~10 μm).

The enhanced transfer we observe for small donor-acceptor separations is not predicted in recent theoretical work (*11*, *12*). These reports concentrate on the effect the cavity has on the photons that mediate the transfer and in doing so ignore the important effect of the cavity on the donor; they appear to assume unit donor oscillator strength. Summarizing their picture, when donor and acceptor are close and transfer is efficient, the cavity has little effect on the evanescent mediating photon, so transfer is unaltered. In contrast, when donor and acceptor are well separated, the mediating photon is real or propagating and strong transfer enhancement is predicted. Unfortunately, transfer is much less likely at these large separations; consequently, observation of this enhancement requires the use of either a high–quality factor cavity (*22*) or a large number of acceptor molecules (*16*, *17*). By assuming unity donor oscillator strength, the theories discussed above miss the important role the cavity plays in modifying the Förster transfer process. The dependence of the Förster process on the donor oscillator strength has been known since the first reports on energy transfer (*9*). With the current interest in the use of photonic materials to control optical processes, it is surprising that enhancing transfer by modifying the donor oscillator strength seems to have been overlooked.

This new understanding can be put to practical effect. In many device architectures, fabrication is simplified by the deposition of active layers containing a random distribution of dye molecules, rather than as an ordered nanostructure. In such systems, the Förster process is likely to be the dominant transfer mechanism because any excited donor will have a number of acceptor molecules in close proximity. Indeed, Förster transfer has already been used to increase the efficiency of light-emitting devices based on organic materials by recouping energy lost to nonradiative triplet states (*3*). This was achieved by transferring the excitation energy from the triplet state to radiative singlet states of dopant dyes. Another application is in solid state polymer dye lasers, Förster transfer being used to spectrally shift the lasing wavelength away from the strong absorption losses of the host materials (*23*). In both these applications, increasing the donor oscillator strength through the use of microcavities resonant at the transfer wavelength could enhance the rate of Förster transfer still further and may be particularly important in lasing schemes where transfer is the rate-limiting step. It is interesting to note that a recent report indicates that in the process of photosynthesis, Förster energy transfer already benefits from increased donor oscillator strength, here brought about by the aggregation of dye molecules (*24*). Our demonstration that Förster energy transfer depends on the local optical environment means that the multiplicity of reports using confining structures to alter spontaneous emission also provide suitable strategies to control energy transfer.

References and Notes

1. J. R. Oppenheimer, *Phys. Rev.* **60**, 158 (1941).
2. R. van Grondelle, J. P. Dekker, T. Gillbro, G. Sundström, *Biochim. Biophys. Acta–Bioenergetics* **1187**, 1 (1994).
3. M. A. Baldo, M. E. Thompson, S. R. Forrest, *Nature* **403**, 750 (2000).
4. A. Dodabalapur *et al.*, *J. Appl. Phys.* **80**, 6954 (1996).
5. K. H. Drexhage, in *Progress in Optics*, E. Wolf, Ed. (North-Holland, Amsterdam, 1974), vol. XII, pp. 163–232.
6. J. M. Gérard *et al.*, *Phys. Rev. Lett.* **81**, 1110 (1998).
7. P. Berman, Ed., *Cavity Quantum Electrodynamics, Advances in Atomic, Molecular and Optical Physics*, suppl. 2 (Academic Press, London, 1994).
8. A. Scherer, T. Doll, E. Yablonovitch, H. O. Everitt, J. A. Higgins, *IEEE J. Light. Technol.* **17**, 1928 (1999).
9. T. Förster, *Disc. Farad. Soc.* **27**, 7 (1959).
10. D. L. Andrews, *Chem. Phys.* **135**, 195 (1989).
11. G. S. Agarwal, S. Dutta Gupta, *Phys. Rev. A* **57**, 667 (1998).
12. T. Kobayashi, Q. Zheng, T. Sekiguchi, *Phys. Rev. A* **52**, 2835 (1995).
13. G. Kurizki, A. Kofman, V. Yudson, *Phys. Rev. A* **53**, R35 (1996).
14. G. Kurizki, A. Z. Genack, *Phys. Rev. Lett.* **61**, 2269 (1988).
15. S. John, J. Wang, *Phys. Rev. A* **43**, 12772 (1991).
16. D. G. Lidzey, D. D. C. Bradley, A. Armitage, S. Walker, M. S. Skolnick, *Science* **288**, 1620 (2000).
17. M. Hopmeier, W. Guss, M. Deussen, E. O. Gobel, R. F. Mahrt, *Phys. Rev. Lett.* **82**, 4118 (1999).
18. E. Fermi, *Rev. Mod. Phys.* **4**, 87 (1932).
19. M. G. Salt, W. L. Barnes, *Opt. Commun.* **166**, 151 (1999).
20. H. Kuhn, D. Möbius, H. Bücher, in *Techniques of Chemistry*, *Physical Methods of Chemistry Part 3B*, A. Weissburger, B. W. Rossiter, Eds. (Wiley-Interscience, New York, 1972), vol. 1, pp. 577–703.
21. P. T. Worthing, R. M. Amos, W. L. Barnes, *Phys. Rev. A* **59**, 865 (1999).
22. L. Folan, S. Arnold, S. Druger, *Chem. Phys. Lett.* **118**, 322 (1985).
23. M. Berggren, A. Dodabalapur, R. E. Slusher, *Appl. Phys. Lett.* **71**, 2230 (1997).
24. J. L. Herek *et al.*, *Biophys. J.* **78**, 2590 (2000).

25. The authors acknowledge the support of the UK Engineering and Physical Sciences Research Council (GR/L43619 and GR/M73903) and the Leverhulme Trust.

20 July 2000; accepted 8 September 2000

Hurricane Disturbance and Tropical Tree Species Diversity

John Vandermeer,[1]* Iñigo Granzow de la Cerda,[2] Douglas Boucher,[4] Ivette Perfecto,[3] Javier Ruiz[5]

The debate over the maintenance of high diversity of tree species in tropical forests centers on the role of tree-fall gaps as a primary source of disturbance. Using a 10-year data series accumulated since Hurricane Joan struck the Caribbean coast of Nicaragua in 1988, we examined the pattern of species accumulation over time and with increased sampling of individuals. Our analysis shows that the pattern after a hurricane differs from the pattern after a simple tree-fall disturbance, and we conclude that pioneers are limited in large disturbances and thus do not suppress other species the way they do in smaller disturbances.

A persistent issue in ecology is how tree species diversity is maintained in tropical rainforests (*1, 2*). Studies have proposed (*3, 4*) and then challenged (*5*) the idea that disturbances, in the form of tree-fall light gaps, set back the process of competitive exclusion, thus conforming to the intermediate disturbance hypothesis (*1*). This hypothesis states that neither very large nor very small disturbances can deter the eventual extinction of species, either through competition or through the disturbance event itself, and that only disturbances of intermediate intensity can have this effect. Central to the intermediate disturbance hypothesis is a higher spe-

[1]Department of Biology, [2]University Herbarium, [3]School of Natural Resources and Environment, University of Michigan, Ann Arbor, MI 48109, USA. [4]Department of Biology, Hood College, Frederick, MD 21701, USA. [5]Universidad de las Regiones Autónomas de la Costa Caribe de Nicaragüense (URACCAN), Bluefields, Nicaragua.

*To whom correspondence should be addressed. E-mail: jvander@umich.edu

Förster Energy Transfer in an Optical Microcavity

Piers Andrew and William L. Barnes

Science **290** (5492), 785-788.
DOI: 10.1126/science.290.5492.785